

# An Experimental Study of a Rotor in Axial Flight

F. Caradonna, E. Henley, M. Silva and S. Huang  
Army Aeroflightdynamics Directorate  
Ames Research Center

N. Komerath, U. Reddy, R. Mahalingam, R. Funk, O. Wong,  
R. Ames, L. Darden, L. Villareal, J. Gregory  
School of Aerospace Engineering  
Georgia Institute of Technology, Atlanta, GA 30332-0150

## Abstract

This paper studies the concept of extracting hover performance from model rotor climb data by extrapolating to the limit of zero climb speed. A 2-bladed rotor is mounted horizontally and tested in the 30' × 31' settling chamber of the Ames 7' × 10' #1 wind tunnel. The collective pitch and tunnel speed are varied. CCD video cameras are used to visualize the flowfield illuminated by pulsed white light sheets. Facility recirculation effects are eliminated at all but the lowest advance ratios. With a steady, non-recirculatory flow, the rotor wake is seen to be fully periodic, with little diffusion and dissipation of the vortices for several rotor cycles. The transition to the far wake is seen to occur through a periodic pairing of the tip vortices, followed by their merging into a single diffuse vortex for each rotor cycle. The number of discrete vortex turns in the near wake before the pairing varies with the thrust coefficient and advance ratio. The climb-extrapolation method appears to be a reliable and practical approach to obtaining performance data which are free of recirculation or facility effects.

## 1 Introduction

The prediction of hover performance to high levels of accuracy is one of the oldest and most fundamental problems in rotor aeromechanics. This is because of:

- the importance of hover performance in the design of helicopters
- the computational problem of predicting accurate and repeatable wakes and

- the experimental problem of attaining clean hover flow-fields devoid of recirculation

This paper is directed at the last aspect of the problem.

For a combination of technical, cost and productivity issues, there are few facilities suitable for hover performance measurement. The measurement of hovering rotor performance requires a very large facility in order to minimize recirculation. Indoor facilities are extremely rare - typically they are large rooms intended for multi-purpose use. Outdoor testing is also difficult because of the great sensitivity to wind effects and the fact that outdoor facilities are usually designed for full-scale testing and often subject to mount interference effects. There is no standard facility for such purposes. Moreover, there are few meaningful comparisons of hover performance measurements between facilities. An excellent example of the potential sensitivity of hover performance to facility configuration is given by Shinoda and Johnson[1]. They show impressive hover performance variations for an S-76 rotor in the 80' × 120' tunnel. There is probably a great deal of uncertainty in most hover performance data, and, therefore, of our predictive ability. In the design process, this problem often contributes to the need to specify large available power margins.

One of the most salient and disturbing features of hover testing is the degree of unsteadiness that is typically observed. The effects and types of flow unsteadiness seen in hover testing have been reviewed by Leishman and Bagai[2]. Flow unsteadiness (typically seen as a meandering in wake visualizations) and performance measurement accuracy are definitely related, but the relationship is not known. The work of Piziali and Felker[3] is one of the few published studies that attempts to quantify and control the effects of unsteadiness. They obtain performance measurements for testing both outdoors and in a treated chamber. In this and other studies, known causes of unsteadiness include recirculation and wind effects. However, unsteadiness

---

\*Copyright©1997 by the American Helicopter Society. Presented at the AHS Technical Specialists' Meeting for Rotorcraft Acoustics and Aerodynamics, Williamsburg, VA, October 28-30, 1997

ness is so ubiquitous that it may also be attributable to inherent wake instability. Such intrinsic unsteadiness could limit our computational expectations and possibilities for facility improvement. On the other hand, if steady flows are practically obtainable, it should be possible to greatly improve experimental repeatability and accuracy and this would lead to computational methods in which we can have the highest confidence.

The work reported on herein is a pilot test of an approach to remove this unsteadiness and to apply practical optical methods for studying the resulting flow. The work involves simulating a climb state in a model rotor appropriately mounted in a wind-tunnel settling chamber. Previous horizontal-axis rotor testing has been performed in a tunnel test-section with the purpose of studying descent flows, as in Reference [4]. The goal here is not only to achieve a steady flow, but to achieve it at an effective climb rate that is low enough to infer the hover performance.

This work is a cooperative effort between the Army Aeroflightdynamics Directorate at Ames Research Center and the Georgia Institute of Technology and was funded by the Ames Directors Discretionary Fund and the Rotorcraft Center of Excellence at GIT.

## 2 Related Work

Work on modeling the rotor wake has continued since the early days of rotorcraft development. Experimental efforts to capture wake structure have been plagued by the difficulty of maintaining periodic flow beyond the first couple of turns of the vortex. Reference [5] states that "in almost every visualization technique, the qualitative aspects of vortex dissipation are quite apparent".

Gray and Brown[6] developed a simple model for the structure of a single-bladed rotor in hover. Samant and Gray[7] extended these studies to document vortex trajectories in the wake of a single-bladed rotor in hover in a double-walled facility. A wake inductor was constructed by trial and error using helium bubble flow visualization to let the contracting wake pass unimpeded over the range of thrust conditions tested. The return flow came either through the annulus outside the inner walls, or through a honeycomb screen located around the wake inductor. Using this set-up, steady periodic vortex trajectories were captured using helium-filled soap bubbles, and later using laser sheets illuminating oil droplets [8]. The region of particle deficit in the vortex core was seen to expand, but the vortex itself was visible as a discrete structure beyond  $1080^\circ$  of vortex age. The trajectories were steady enough to permit measurement of all three components of velocity with a laser velocimeter, one component at a time, using the measured core trajectory to locate measurement points at specified vortex age. Core velocity measurements

were performed using this technique, using sub-micron incense smoke particles which stayed entrained in the core, at upto  $180^\circ$  of vortex age, with negligible unsteadiness as seen from histograms of velocity within narrow intervals of rotor azimuth. Even the secondary structures due to rolling-up vortex sheets were visible and repeatable in the profiles of axial and tangential velocity across the vortex core.

When experiments were conducted with a slightly larger rotor blade radius in the same facility [9], it was found to be impossible to keep the unsteadiness low at some conditions. Laser sheet flow visualization showed the tip vortex escaping the lip of the wake inductor, interacting with the walls, and returning to the vicinity of the tip path plane, outside the wake, causing severe unsteadiness of the vortex trajectory. The key point here is that the tip vortices remain strong for long vortex ages in hover tests, so that their interaction with facility walls causes a feedback to the rotor tip path plane, even when the walls are thought to be "sufficiently" far away.

In forward flight experiments, the rotor tip vortex has been seen to persist for substantially longer vortex age. The HART rotor flow visualization experiments conducted at the DNW tunnel (see Reference[10] for a recent discussion) show strong, steady vortex cores (as seen from the particle deficit in the core), persisting well beyond  $180^\circ$  of vortex age. Experiments at the Georgia Tech  $7' \times 9'$  wind tunnel show core axial velocities persisting at levels comparable to the peak tangential velocity, for over  $240^\circ$  of vortex age with little unsteadiness [11, 12]. The key difference appears to be that wake recirculation is eliminated by operating at a forward-flight advance ratio where the wake gets completely swept downstream without interacting with the facility walls.

Diffusion of the vorticity has been proposed by some researchers as a mechanism for the apparent decay of vortex core velocity profiles obtained from hover flowfields. Reliable data on vortex diffusion are sparse. Efforts to measure such quantities appear to have encountered substantial levels of vortex unsteadiness due to facility wall effects, and failed to perform conditional sampling before ensemble averaging the data. As pointed out by Conlisk[13], the time scales for diffusion of vorticity from a vortex are extremely long, (see exact solution in Schlichting[14]), a fact manifested in the persistence of fixed-wing tip vortices for durations of the order of a minute after an aircraft passes[15]. If turbulent diffusion is responsible for the rapid decay of vortex velocities reported in hover (where the ambient flow has no turbulence), then the vortex should decay much faster in forward flight experiments in a wind tunnel, where the freestream has a wide range of turbulence scales. The well established observation of vortices persisting to large ages in wind tunnels conflicts with the idea of turbulent diffusion.

These experiences show the extreme difficulties in conducting interference-free hover testing, and the severe unsteadiness resulting from vortex interaction with facility walls. The question posed in this paper is whether the hover condition can be extrapolated as the limiting case of zero climb, and hence the unsteadiness in the facility prevented from obscuring the physics of the rotor wake. The results are surprising, in that the mechanism of transition to the far wake is clearly visible as a deterministic and repeatable phenomenon.

### 3 The Experiment

#### 3.1 Physical Layout and Instrumentation

The idea of this test is to operate a model rotor in a low-speed axial free-stream. The axial state (i.e. climb rate) is achieved by orienting the rotor axis horizontally and locating it in a wind-tunnel settling chamber, where the free-stream would be low and wall effects minimized by the chamber size. The present test used a 7' diameter model rotor mounted horizontally in the settling chamber of the 7' x 10' #1 wind-tunnel at Ames Research Center. The cross-section of the settling chamber is 30' x 31'. A sketch of the set-up is shown in Figure 1 below.

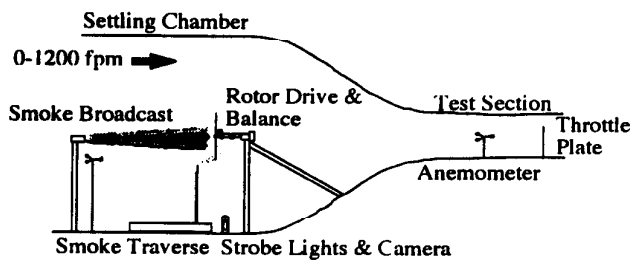


Figure 1: A sketch of the axial-rotor test set-up in the Army/Ames 7' x 10' Wind Tunnel

This is a low-speed tunnel with a maximum test section velocity of about 300 fps (with a clean tunnel). With a contraction ratio of 13.2857, the tunnel can simulate a maximum rate-of-climb approaching 60 fps. However, this test requires operation at much lower speeds. At these low velocities the tunnel drive fan required less power than the model rotor and speed control was lost. This required installing baffles in the tunnel test section in the later test phases.

The 7' x 10' tunnel has recently been modified by the addition of 4 sets of anti-turbulence screens located upstream of the settling chamber turning vanes. (Usually, turbulence screens are located in a settling chamber.

However, the present installation locates the screens upstream of the turning vanes to enable use of the chamber for rotor testing.) These screens have substantially improved the turbulence measurements in the test section flow. There have been no turbulence measurements in the settling chamber. However, smoke visualization has revealed no obvious non-uniformities or swirl.

The low settling chamber velocities are difficult to measure accurately. Therefore velocity measurements were mostly made in the test section. The lower velocities were measured using an anemometer. Anemometer measurements were also made in the settling chamber. Checks of the settling chamber velocity were performed by timing the passage of smoke puffs over a known distance.

Mounting the rotor in the setting chamber required design and fabrication of a large, tripod-like, mounting system that was fixed to the primary tunnel structure. This mount system centered the rotor in the settling chamber cross-section at a point about 8' upstream of the beginning of the contraction section. (This location was chosen primarily for safety reasons as it placed the rotor well within the steel section of the tunnel wall.) The horizontal-axis mode of rotor operation required the use of the ARTS (Army Rotorcraft Test System) drive system, which was designed for operation in a range of orientations. This system is designed for driving much larger rotors with power requirements in excess of 400 HP. For the present work it was necessary to modify the ARTS drive by replacing the first gear-reduction stage with an adapter that permitted mounting of two smaller drive motors (Able 90 HP motors). Because of the small rotor size, the normal ARTS balance was replaced by a smaller balance from the Army RWTS (Rotary Wing Test Stand). This balance was also larger than desired. The rotor drive shaft passes directly through the balance and the bearings (located on the metric side of the balance) heat the inner balance. This heating combined with the low load sensitivity results in significant thermal drift, and required frequent rezeroing of the load readings.

Figure 2 shows a photograph of the stand mounted in the settling chamber. The rotor is a model AH-1G, mounted on a teetering hub and with a full swashplate control. Following a complete track and balance of the rotor the swashplate cyclic control was disabled. The primary test instrumentation was the rotor balance and shaft torque. Real-time balance element and torque data were continuously displayed (primarily for system health monitoring), with the frequency spectra being displayed at new run conditions. Averaged values of thrust and torque were displayed and recorded continuously, together with the rotor hover figure-of-merit (FM). The figure-of-merit display was especially valuable because its extreme sensitivity magnified the effects of thermal drift. The steadiness of this figure-of-merit output was used as an indicator

of the system having attained thermal equilibrium. Data were not recorded until FM drift was stabilized, which was a lengthy process requiring about 2 hours of operation. Subsequent rezeroing of the data, which requires stopping the rotor, was performed at regular intervals thereafter and many data repeats were made throughout the period of the test. In this manner, a definite warm-up, run and rezeroing sequence was established and repeated many times over in order to observe the thermal/mechanical/electrical behavior of the system and enable recognition of data anomalies. This permitted the acquisition of data with sufficient accuracy and repeatability for the present purposes.

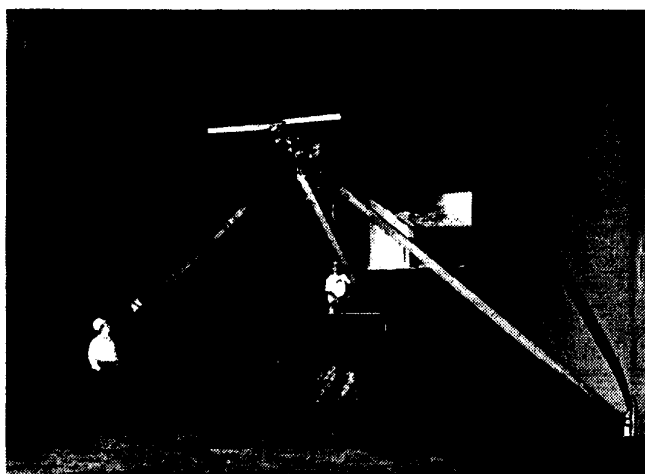


Figure 2: A photograph of the axial-rotor test set-up

### 3.2 Flow visualization set-up

A major part of this test was concerned with observing the effect of run condition on the state of the rotor wake. For this purpose the wake was visualized using theatrical smoke and a white light-sheet system. A general smoke broadcasting system was deployed far upstream of the rotor for visualizing the overall wake region and providing visible particles for field velocity measurements. Closer to the rotor, a single-point smoke source was deployed for visualizing the tip vortices. Since the flow streamlines vary considerably with climb rate, the near-rotor smoke wand was mounted on a remotely controlled traverse. In a near-hover state the smoke source was located very close to the edge of the rotor disc (slightly upstream and about 8" outboard), while for high climb rates, it was necessary to move the source as much as 10' upstream.

The smoke was illuminated with a light sheet using a portable, stroboscopic light source. The illuminated wake region was recorded directly on video tape using a pair of intensified commercial grade CCD video cameras viewing

approximately perpendicular to the light sheet. A dual-light, dual-camera system was required for planar velocity measurements (not addressed in this paper). A schematic of this imaging set-up in the settling chamber is shown in Figure 3.

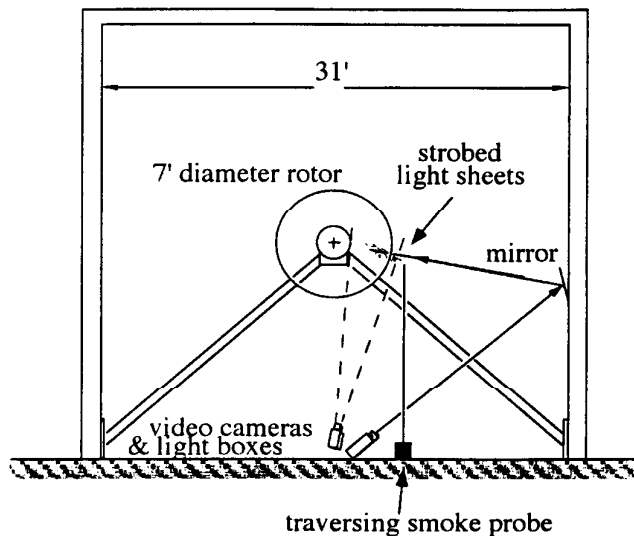


Figure 3: A cross-section of the test set-up showing the flow-visualization arrangement

The light to measurement plane and camera to measurement plane distances exceeded 15 ft. The flow visualization area surpassed  $6.5' \times 5'$  but could also be zoomed in to view vortices. The strobe lights were either synchronized to the rotor or externally triggered to pulse at video framing rate (29.97 Hz). The two light sheets were aligned to coincide in the region of interest. The lights and camera shutters were synchronized, and their phase with respect to the rotor was varied.

### 3.3 Tracking Vortex Trajectories

A sequence of frames at approximately  $15^\circ$  intervals, over a period of several rotor cycles, were digitized from a section of the flow visualization video. Given the inclination of the light sheet, the instant a reflection of the rotorblade is seen in the light sheet was used as the starting azimuth for tracking the wake. The vortices appear as dark regions (since the seed particles are centrifuged out of the vortex core) surrounded by a bright region of smoke. The location of vortex centers was determined as pixel coordinates in a  $640 \times 480$  image, to within 1 pixel accuracy. These were then converted to physical coordinates with the rotor hub location as origin using a grid board recorded prior to the run. Vortices shed from the two blades were tracked separately.

## 4 Results

Initial testing was aimed at measuring the effect of climb velocity on the rotor efficiency and ascertaining the lower climb-rate limits of such testing; that is, how closely a true hover can be approached and the extent to which true hover performance can be inferred from climb data.

Initial operation of the rotor, with the tunnel drive system turned off and the tunnel test-section in a clean condition, was aimed at obtaining sweeps of the rotor collective. These sweeps extended from zero thrust to the onset of an obvious stall flutter (determined by torsional loads and the rotor sound). This flutter state was the only condition for which we were able to detect any flow unsteadiness. That is, it was immediately found that the axial mount of the rotor did eliminate wake unsteadiness. This was ascertained by visualization of the tip vortices and also by examination of the spectra of the balance gages. It was found that the frequency content of the balance gages (both axial and side gages) was essentially independent of the rotor collective. This implies that aerodynamics is not a forcing function for the system and this is consistent with the observed vortex behavior (to be shown later).

The unusual steadiness of the flow at all collectives is undoubtedly related to the rotor driving the tunnel flow and simulating a climb condition. Of course, the effective rate-of-climb is a function of the rotor collective and is therefore not fixed throughout a collective sweep. In order to enable a fixed climb rate throughout the collective sweep it was necessary to decouple the tunnel speed from the rotor power. This was done by installing a large flat-plate to act as a throttle in the tunnel test section and then operating the tunnel drive fan such that a fixed rate-of-climb is obtained throughout the collective sweep.

Figure 4 shows a plot of the measured hover figure-of-merit vs. collective at a fixed climb rate of 3.5 fps. These data is marked by an uncertainty band that is about 3% wide. The width of this band is due to the previously mentioned rotor/balance mismatch and the resulting thermal sensitivity. (We estimate that 60 to 70% of this uncertainty results from thermal drift, while the remainder is random scatter.) This error band is narrow enough to discern major figure-of-merit trends and is sufficient for present goals. The important aspect of this data is that the uncertainty arises solely from instrumentation sources and this can be easily corrected in future tests. The flow itself is completely steady and is not a contributor to the data uncertainty.

Having determined that steady, deterministic flows appear to be normal for low climb rates, we now consider the overall trend of performance with climb-rate. Figure 5 shows a plot of the hover figure-of-merit for axial velocities ranging from 0 to 15 fps. (The lower velocities are obtained using the aforementioned throttling of the tunnel). The

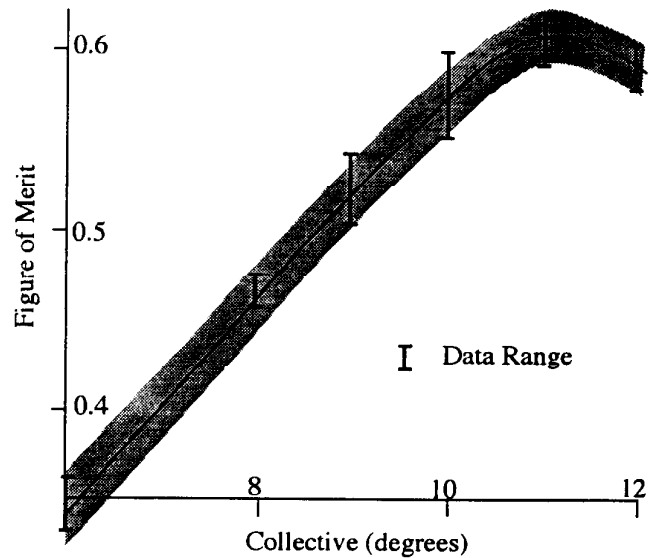


Figure 4: Rotor Figure of Merit as a function of collective at a climb-rate of 3.5 fps

plot is marked by an essentially linear variation of hover figure-of-merit with climb rate for all but the lowest climb rates. The deviation of FM from the linear trend occurs precipitously at about 3 fps. At this point the FM trend reverses suddenly and decreases steeply with decreasing climb-rate (axial velocity). Coincidentally with the reversal of the FM trend the flow ceases to be steady. At this point the balance gages show a sharp increase in both the 2/rev and 6/rev loads and this unsteadiness increases with decreasing axial velocity. At this point too, the flow visualization ceases to be steady. It is difficult to determine whether this unsteadiness involves major changes in the tip-vortex trajectories because of unsteady changes in the smoke path. The smoke path changes indicate that major flow recirculation has started. In addition, the data error bands become much wider in this region, indicating that a new source of uncertainty has arisen.

Clearly this low speed region is not a trustworthy simulation of the hover flow state. The most meaningful information to be gleaned from this low speed region is the magnitude of performance error that can occur. It is reasonable to assume that the true hover performance is obtained by extrapolating the linear climb trend to zero climb-rate. This results in an FM of about 0.65. The actual value of FM that is measured at zero climb is about 0.55 - a probable error of 10%, which is quite extreme. The degree of unsteadiness that is occurring here would probably be recognized as being excessive under most test situations. However, all hover tests involve some degree of unsteadiness. The important question is, how much unsteadiness

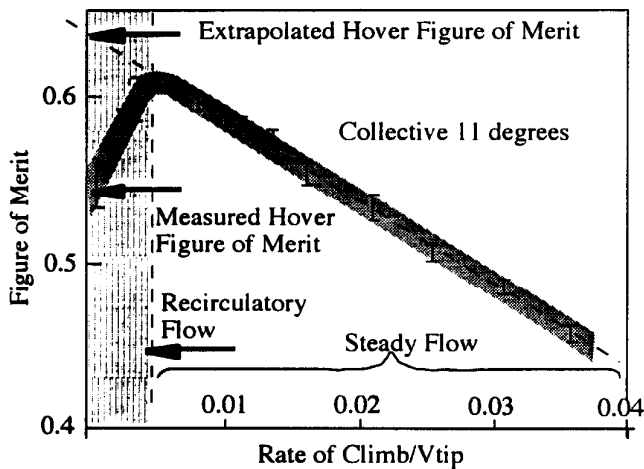


Figure 5: The effect of climb-rate on measured rotor performance

(or recirculation) is acceptable? In view of the possible magnitude of the error, the probable answer to that question is that no unsteadiness should be acceptable until we can quantify its effect on performance accuracy. This is exceedingly difficult and experimentalists are often forced to take what they can get. The approach of extrapolating low climb-rate data to hover is a method that is free of this uncertainty.

The primary method of ascertaining the flow steadiness has been to observe the tip vortex flow visualization. However, the steadiness and repeatability of these visualizations have also permitted the observation of vortex behavior that have not (to the authors' knowledge) been previously reported. It is usually reported that rotor wakes appear to dissipate by an instability growth process that is implied to be stochastic in nature. This is not, however, what has been observed in the visualizations of this particular rotor setup.

Figure 6 shows a sequence of images of the tip-vortex development at a rotor collective of  $9^\circ$  and a climb rate of 3.5 fps. The vortices from the two blades are identified by their numbers, an odd numbered vortex belonging to one blade and even numbered to the other. The time between successive frames is not constant, but was chosen to show the progression of the pairing phenomena. The first frame shows two clear vortices, marked "3" and "4". In the next frame, vortex "3" has begun to roll up with "4". This process continues in the next two frames, until "3" and "4" have essentially interchanged positions while moving downstream. In the final frame, the rolled-up pair have begun to lose identity, with their core particle deficits disappearing.

The notable aspect of this visualization is that the vortex trajectories do not appear to follow a path whose

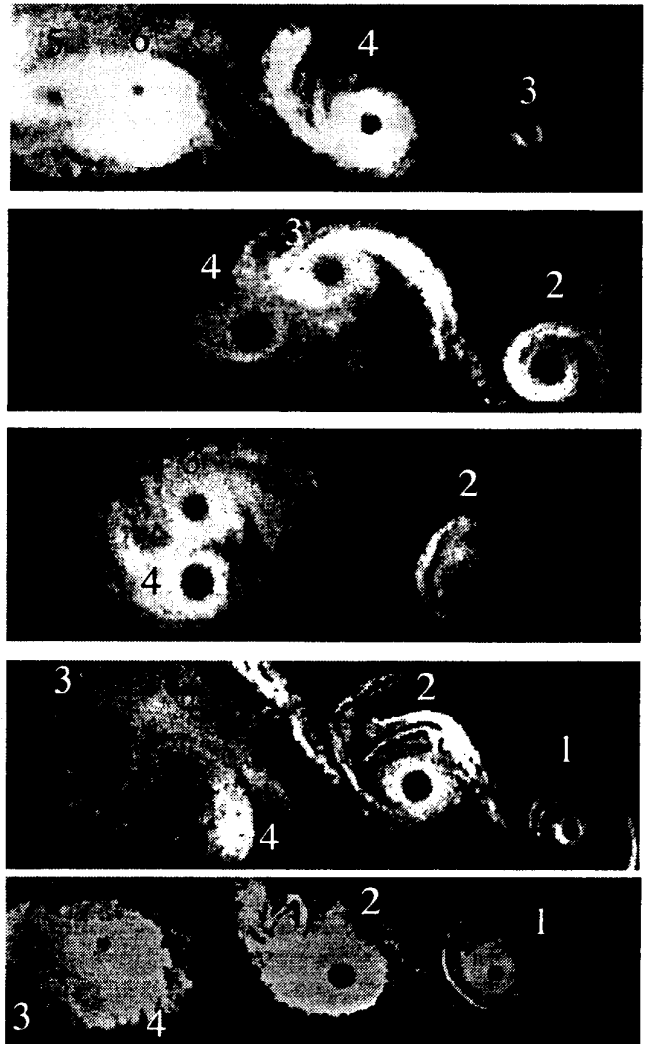


Figure 6: Sequence of vortex roll-up from the individual blades,  $9^\circ$  collective, 3.5 fps climb rate

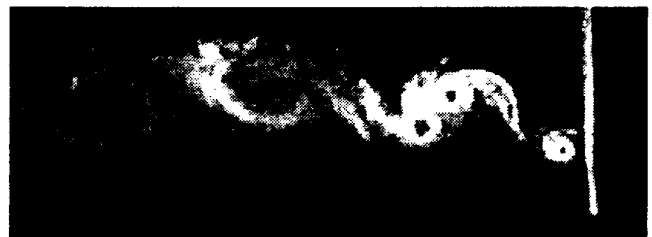


Figure 7: Formation of single diffuse vortex by interaction of vortices from individual blades,  $7.5^\circ$  collective, 3.5 fps climb rate



Figure 8: Flow-visualization at 24.2 fps climb rate, 7.5° collective

contraction increases monotonically with time. Beyond a certain age, the vortex trajectory tends to expand radially. Moreover, the spacing between tip vortices also seems to change. Such vortex “expansions” have been noted in many previous tests and visualizations and frequently attributed to being some manifestation of an instability process. Examination of the wake at various points in time has revealed that the vortex trajectory disturbances seen here are highly repeatable between rotor revolutions. The vortex “expansion” was seen to be a result of adjacent tip vortices beginning to pair together and spiral about each other. This process culminates in a complete merging of the two tip vortices into a single, more diffuse vortex as seen in Figure 7. This phenomenon has been seen over the entire range of collectives and free-stream axial velocities. The location of vortex pairing changes with the rotor collective angle and the advance ratio in climb. Figure 8 shows the vortex shedding pattern at a high climb rate of 24.2 fps. The spacing between successive vortices remains large for several rotor cycles so that several clear and discrete vortices are seen. Also, at high climb-rates vortex pairing is considerably delayed due to larger separation between the vortex helices.

The vortex pairing process has been quantified by trajectory tracking. The trajectories of the tip vortices for 6°, 7.5° and 9° collective at a climb rate of 3.5 fps are shown in Figure 9. The tip vortex trajectories from the two blades are offset by 180° and it is clear that they are influencing each other. The first intersection of the  $x/R$  curves of the two vortices indicates the beginning of the vortex pairing process. Subsequent crossings indicate the rotation of the two vortices about each other. A comparison of the 6° and 9° case clearly shows that the initiation of the wake roll-up is delayed by increasing the collective. The spiraling of the vortices around one another brings them closer and eventually they form a diffuse circulatory region indicated by the merger of the trajectories from the two blades.

Figure 10 shows the vortex trajectories for three climb rates (3.5fps, 6.8fps and 9.6 fps) at a fixed collective of 11°. These trajectories do not show significant differences since the effective inflow rates (climb and induced velocity) in the settling chamber are not substantially different. The

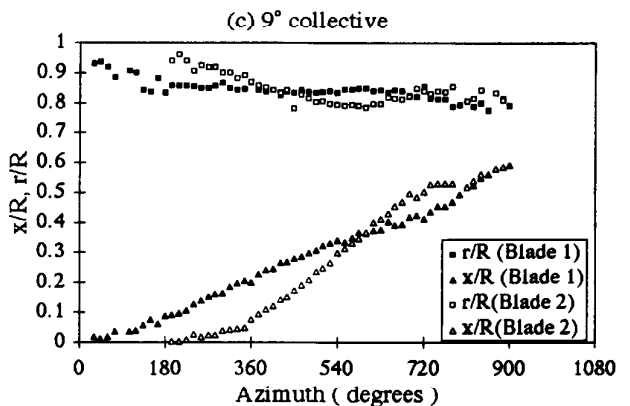
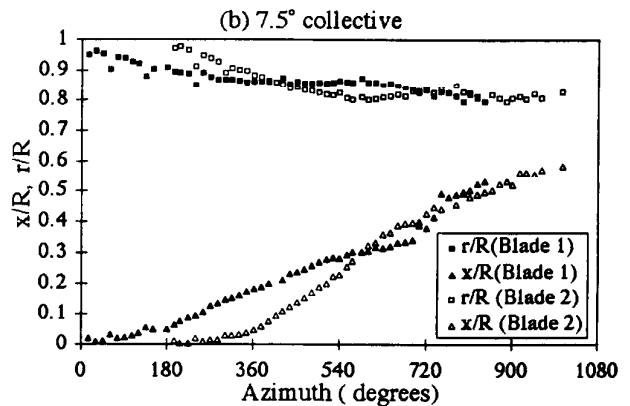
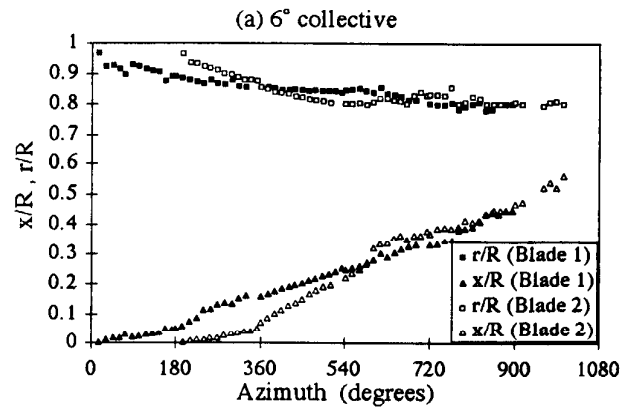


Figure 9: The effect of collective on wake geometry at 3.5 fps

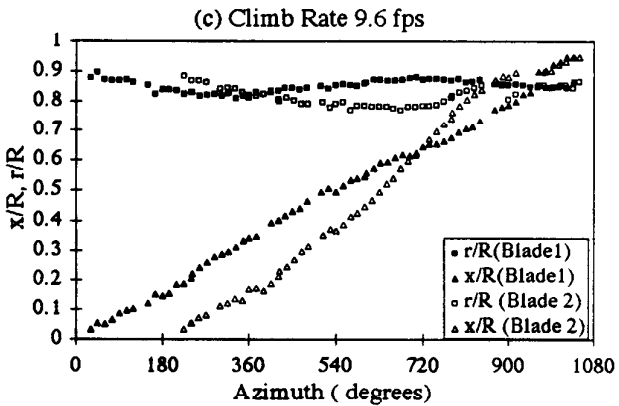
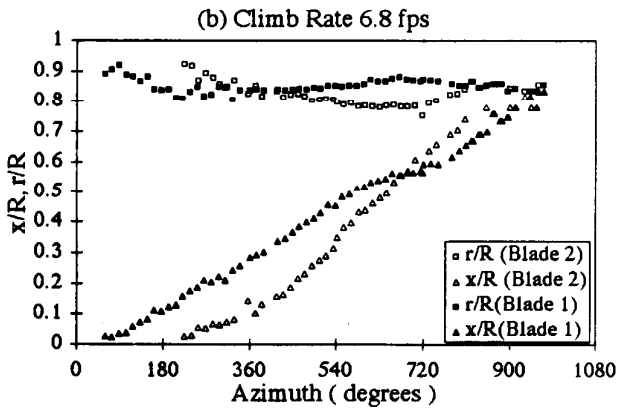
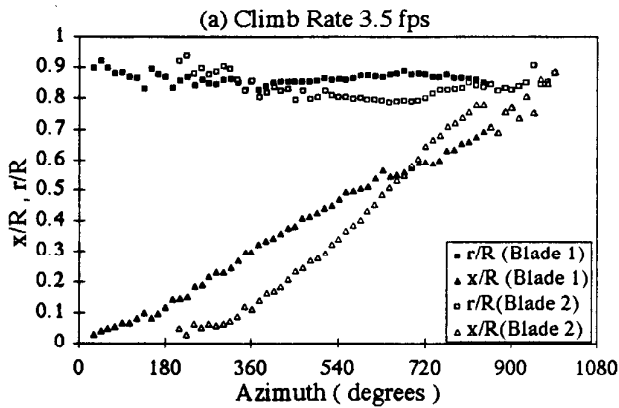


Figure 10: The effect of climb-rate on wake geometry at 11° collective

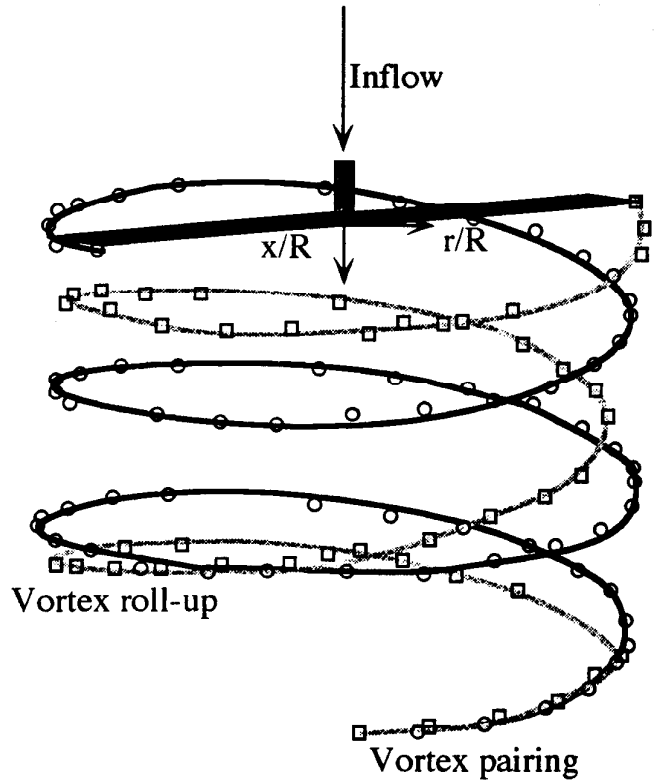


Figure 11: 3-D tip-vortex geometry at 11° and 9.6fps. The axial direction has been stretched by a factor of 1.5 for clarity

$x/R$  curve from the two blades intersect at an azimuth of approximately 580° for the 6° case in Figure 9(a) and 680° for the 11° case in Figure 10(a) i.e. a delay of about 100° of rotor azimuth.

The trajectories at 11° collective and climb-rate 9.6 fps are represented in 3D vortex-trajectory form in Figure 11. The crossing of the two trajectories indicates the commencement of the roll-up process. Vortex pairing is evident in the merger of the two helical trajectories.

Following these observations, we have examined a number of visualizations from other tests and we find the vortex pairing phenomena to be a fairly common occurrence. Probably the finest photograph we have found of the phenomena was acquired by Dr. Reinert Mueller as a part of his dissertation work at the Rheinisch-Westfallisch Technische Hochschule, Aachen [16]. This visualization, shown in Figure 12, employs theatrical smoke ejected from the tips of a two-bladed rotor. The merging of the two tip vortices into a single diffuse vortex is clearly seen in this figure. This merging process is not uncommon or unique to the present test. It is surprising, therefore, that the phenomenon has not been recognized in the past. The most



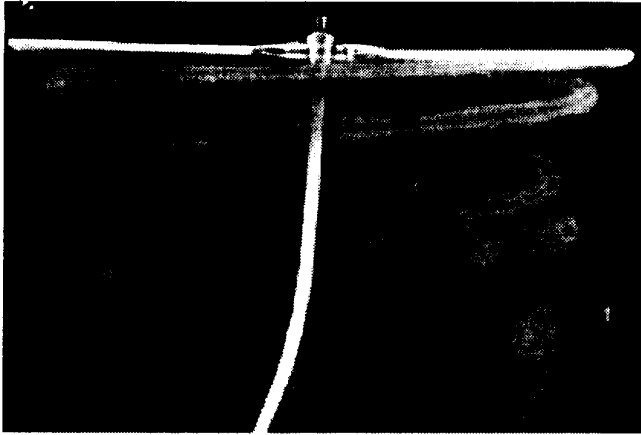


Figure 12: Merging of tip vortices from a two-bladed rotor as visualized by Dr. Reinert Mueller. Reprinted with permission

probable explanation is the characteristic unsteadiness of most hover testing.

## 5 Concluding Remarks

The operation of a rotor horizontally in a wind-tunnel settling chamber is an excellent method of simulating rotor climb flows. We have found that there is a critical free-stream flow velocity, above which the chamber flow has no recirculation and the total rotor/wake flow is remarkably steady. This critical free-stream speed is fairly low and at these speeds the resulting wake behavior (contractions and rotor-wake proximities) closely resembles hover. Throughout the entire steady flow region, the trend of rotor power (measured using the hover figure-of-merit) as a function of climb rate is essentially linear. This smooth performance trend, combined with the low value of critical velocity, suggests strongly that an extrapolation of the figure-of-merit to hover to a zero climb-rate would provide a highly accurate and repeatable (in time and also between facilities) measure of hover performance.

The behavior of the performance trend below the critical velocity suggests that this performance extrapolation is a necessity. Below the critical velocity, recirculation commences, accompanied by unsteady flow and a sudden reversal of the performance trend. The measured figure-of-merit at a zero climb differs from the extrapolated value by an amount that exceeds any conceivable measurement or extrapolation error. Of the two methods of performance measurement, direct vs. extrapolated measurement, the latter is certainly the more trustworthy, because it is derived from steady, deterministic data.

The low climb-rate data obtained above the critical

velocity is notable for being highly steady. This steadiness permitted the observation of a vortex pairing phenomenon wherein tip vortices ultimately merge, producing a single vortex rather than two. This merging process is highly repeatable. The steadiness of the wake data seen in low rate-of-climb suggests that most wake unsteadiness seen in rotor hover testing may be due to inflow contamination (say, by recirculation or ambient wind) rather than being an intrinsic instability of the wake. It further suggests that we should not accept stochastic hover results (at least for isolated rotor testing) as being unavoidable. The present extrapolated climb method is a probable way to avoid such flow quality questions in the future.

The ability to produce steady, deterministic rotor/wake flows experimentally implies that such flows can also be computed. This should extend to the ability to predict the pairing process. Such computations will certainly require large computing resources (by today's standards), but it seems clear that it can be done. The availability of steady flows such as have been obtained should provide us with a standard by which computational methods can be validated. It is possible that the wake structure can be extrapolated to a hover state and these wakes used for hover method validations. However, data from the climb tests should also be reproducible computationally. An ability to successfully compute such climb states would imply an ability to predict the hover state.

This work has been a pilot effort to determine the utility of performing rotor tests with axial free-stream velocities. The method is very effective and practical and should be further developed. The steadiness of the resulting flow data provides excellent performance data. The steady flow in the settling chamber does break down at a low climb rate. However, this rate-of-climb is low enough that data from the steady flow region can be extrapolated accurately to hover. However, the unsteady region may also be of some significance. Within this region there exists both a wide range of flow unsteadiness and a good performance measurement standard (namely the performance extrapolated from the steady flow region.) This provides a unique opportunity to quantify the effect of unsteadiness on performance measurement accuracy. Such relationships may be applicable to other facilities and greatly increase their utility.

## 6 Acknowledgements

The Georgia Tech teams participation in this effort was supported under the NASA/Army NTRC Rotorcraft Center of Excellence. Dr. Yung Yu and Dr. T.L. Doligalski are the Technical Monitors. The authors would like to mention that this effort would not have been possible without the aid of Marios Pizza and Italian Restaurant.

## References

- [1] Shinoda, P., and Johnson, W., "Performance Results from a Test of an S-76 Rotor in the NASA Ames 80- by 120- Foot Wind Tunnel", AIAA -93-3414, AIAA Applied Aerodynamics Conference, August 9- 11, 1993, Monterey, CA
- [2] Leishman, J.G. and Bagai, A., "Challenges in Understanding the Vortex Dynamics of Helicopter Rotor Wakes", AIAA-96-1957, 27th AIAA Fluid Dynamics Conference, June 17-20, 1996, New Orleans, LA
- [3] Piziali, R.A. and Felker, F.F., "Reduction of Unsteady Recirculation in Hovering Model Helicopter Rotor Testing", *Journal of the American Helicopter Society*, January, 1987
- [4] Moedersheim, E., Dagher, M., and Leishman, J.G., "Flow Visualization of Rotor Wakes Using Shadowgraph and Schlieren Techniques", Paper 31, 20th European Rotorcraft Forum, October, 1994, Amsterdam, The Netherlands
- [5] Stepniewski, W.Z., and Keys, C.N., "Rotary-Wing Aerodynamics". Dover Publications, Inc., New York, 1984.
- [6] Gray, R.B., Brown, G.W., "A Vortex Wake Analysis of a Single-Bladed Hovering Rotor and a Comparison with Experimental Data", AGARD-CP 111, September 1972.
- [7] Samant, S.S., Gray, R.B., "A Semi-Empirical Correction for the Vortex Core Effect on Hovering Rotor Wake Geometries", *Proceedings of the 33rd Annual Forum of the American Helicopter Society*, Washington, D.C., May 1977.
- [8] Thompson, T.L., Komerath, N.M., and Gray, R.B., "Visualization and Measurement of the Tip Vortex Core of a Rotor Blade in Hover", *Journal of Aircraft*, Vol. 25, No. 12, December 1988, pp. 1113 - 1121.
- [9] Komerath, N.M., Liou, S-G., Hyun, J-S., "Flowfield of a Swept Blade Tip at High Pitch Angles", AIAA 91-0704, *Aerospace Sciences Meeting*, Jan. '91.
- [10] Tung, C., Yu, Y., and Low, S., "The Aerodynamic Aspect of Blade / Vortex Interaction (BVI)", *Invited Paper*, AIAA 96-2010, June 1996.
- [11] Liou, S.G., Komerath, N.M., and McMahan, H.M., "Measurement of Transient Vortex-Surface Interaction Phenomena", *AIAA Journal*, Vol, 28, No. 6, June 1990, p. 975-981.
- [12] Mahalingam, R., Komerath, N.M., "Rotor Tip-Vortex/ Airframe Collision Effects on the Vortex and Airframe", AIAA 96-2013, June 1996.
- [13] Conlisk, A. T., Ohio State University, Private Communication, 1997.
- [14] Schlichting, H., "Boundary Layer Theory", 6th Edition, McGraw-Hill.
- [15] Rossow, V.J., "Wake-Vortex Separation Distances When Flight-Path Corridors are Constrained", AIAA 96-2500-CP, June 1996.
- [16] Dipl-Ing. Mueller, R., "Der Einfluss von Winglets an Rotorblattspitzen auf die Stromungsverhältnisse am Hubschrauberrotor, Eine experimentelle und theoretische Untersuchung", Reihe 12, *Verkehrstechnik / Fahrzeugtechnik*, Nr. 108, VDI Verlag.